energies

MDPI

Article

Portable Mobile Gait Monitor System Based on Triboelectric Nanogenerator for Monitoring Gait and Powering Electronics

Yupeng Mao [1,*], Yongsheng Zhu [1], Tianming Zhao [2], Changjun Jia [1], Xiao Wang [3] and Qi Wang [2,*]

[1] Physical Education Department, Northeastern University, Shenyang 110819, China; 2001276@stu.neu.edu.cn (Y.Z.); 2071367@stu.neu.edu.cn (C.J.)
[2] College of Sciences, Northeastern University, Shenyang 110819, China; zhaotm@stumail.neu.edu.cn
[3] College of Physical Education, Chongqing University, Chongqing 400030, China; wangxiao278@cqu.edu.cn
* Correspondence: maoyupeng@pe.neu.edu.cn (Y.M.); wangqi@mail.neu.edu.cn (Q.W.)

Abstract: A self-powered portable triboelectric nanogenerator (TENG) is used to collect biomechanical energy and monitor the human motion, which is the new development trend in portable devices. We have developed a self-powered portable triboelectric nanogenerator, which is used in human motion energy collection and monitoring mobile gait and stability capability. The materials involved are common PTFE and aluminum foil, acting as a frictional layer, which can output electrical signals based on the triboelectric effect. Moreover, 3D printing technology is used to build the optimized structure of the nanogenerator, which has significantly improved its performance. TENG is conveniently integrated with commercial sport shoes, monitoring the gait and stability of multiple human motions, being strategically placed at the immediate point of motion during the respective process. The presented equipment uses a low-frequency stabilized voltage output system to provide power for the wearable miniature electronic device, while stabilizing the voltage output, in order to effectively prevent voltage overload. The interdisciplinary research has provided more application prospects for nanogenerators regarding self-powered module device integration.

Keywords: self-powered; nanogenerators; human mechanical energy collection; sport monitoring

Citation: Mao, Y.; Zhu, Y.; Zhao, T.; Jia, C.; Wang, X.; Wang, Q. Portable Mobile Gait Monitor System Based on Triboelectric Nanogenerator for Monitoring Gait and Powering Electronics. *Energies* **2021**, *14*, 4996. https://doi.org/10.3390/en14164996

Academic Editor: Abdessattar Abdelkefi

Received: 15 July 2021
Accepted: 11 August 2021
Published: 14 August 2021

1. Introduction

Energy is a kind of physical resource that enables humanity in so many ways. With the increase of consumable devices and their functions in daily life, more energy is required to satisfy the respective demands [1–4]. Considering that humanity is fully aware of the consequences of non-renewable energy exhaustion for the planet, we should use renewable energy sources as much as possible in order to satisfy these increasing demands [5]. Renewable forms of energy commonly include solar energy, wind energy, hydroenergy, geothermal energy, mechanical energy, and so on. Specifically, the mechanical energy belongs to a good-quality resource, because it is not limited by time, place, or other objective factors [6–10]. The process of human motion is the most frequent source of mechanical energy, which is sustainable and easy to obtain [11–17]. As wearable devices are continuously developing, people can use them to collect energy for their daily needs [18–24]. In recent years, TENG has attracted broad attention, as it can transform the ubiquitous mechanical energy into electrical energy. The developments of TENG technology have led more widely to applications of nanogenerators in various fields. Compared with electrostatic, piezoelectricity, and electromagnetism, TENG has the functions of low cost, light weight, self-power, and blue energy collection, among others [25]. Meanwhile, TENG can be considered as a promising portable biomechanical energy harvesting platform [26,27]. TENG should also serve more potential applications and demands to improve its power generation performance [28–32]. A possible method is to enlarge the friction area and increase the friction time to improve the electricity generation performance of TENG. The output of TENG is mainly related to contact area [33]. Therefore, a concave-convex TENG

is designed by us to improve the output, which increases the contact area. Hence, the use of other materials on the friction layer and improving working modes are the keys to improving its working performance [34,35].

Additionally, studies have indicated that over one-third of traumas of over 65-year-old men and women worldwide are caused by accident falls. As people grow older and up to over 80 years old, they will have accident falls, at a high probability, every year. This may lead to hospitalization or even death [36–39]. Studies have shown that myasthenia and bad balance are the key factors in fall incidents. An appropriate sport monitoring device, focused on the mobile gaits and stability capabilities in human motion processes, is one of the core plans to prevent falls [40–44]. Therefore, the development of a portable mobile gait monitor system, with an optimized operation mode and improved performance of human motion mechanical energy collection and transformation into electrical energy, is a necessity. Furthermore, it should be capable of monitoring and potentially preventing accidental falls, based on gaits and stability monitoring, which is of great significance to the application promotion of TENG in various fields.

We have designed and built a self-powered portable triboelectric nanogenerator, which is named a portable mobile gait monitor system; this portable mobile gait monitor system can be used to collect human motion energy and monitor mobile gaits and stability. The materials are common PTFE and aluminum foil, used in the fraction layer, which outputs electric signals, based on the triboelectric effect. 3D printing technology is adopted to build an optimized supporting structure, which improves the working mode of the nanogenerator [34,35]. Owing to the increasing contact area, the output is 5.5 times higher than the common contraction-separation TENG. Here, human motion mechanical energy is harvested and transformed into electrical energy, while the gait and stability of multiple human movements are also monitored at the immediate location of the foot base, during the motion processes. This function has enhanced the motion monitoring aspect, as used for preventing falls. A low-frequency stabilized voltage output system is used to stabilize voltage output, so as to provide appropriate power to wearable miniature electronic devices. This interdisciplinary research has provided more application possibilities of nanogenerators' integration into self-powered module devices.

2. Materials and Methods

2.1. Materials

PTFE films (0.5 mm) and Al foils (0.3 mm) were bought from Colleague hareware, Shanghai, China. PLA wires for 3D printing were purchased from Shenzhen Aurora Technique Co., LTD, Shenzhen, China. Emery papers (1200 mesh) were bought from common hardware store.

2.2. Methods

The TENG with optimized structure is redesigned with a new structure and new methods. Firstly, the concave-convex structure is fabricated by a 3D printing machine. Then, the PTFE films and Al foils are cut into pieces after polishing for 60 s. Finally, the PTFE films and Al foils with treatment are pasted on the surface of the concave-convex structure. It is noticed that the TENG without optimization is fabricated with a sandwich structure and materials without treatment.

2.3. Test

The data of properties and applications testing of TENG are tested by an oscilloscope (sto1102c, micsig, produced by Shenzhen China). The properties of parts are tested by improved pulley block and step motor. In practical testing, TENG with optimized structure and TENG with sandwich structure are implanted into shoe soles, respectively, which are prepared for the performance test. For satisfying the requirements of stable power supply with modern microelectronics, we design a low-powered voltage regulator module that can transfer unstable electric pulses into stable output. By integrating with this low-

powered voltage regulator module, the TENG with optimized structure can actively drive the GPS module.

3. Results

The development of intelligent sport is dependent on data collection and monitoring in a reasonable and effective way. With the development of technologies, the electric consumption of one electronic equipment becomes lower; however, the monitoring system integrated with lots of sensors still requires large power supplies [45,46]. Therefore, the biggest issue in sport monitoring is that a battery with a short lifespan can lead to high-cost maintenance and environmental pollution. However, the battery power supply could be replaced when the nanogenerator was born, making it possible to monitor sport with more convenience [47]. Herein, TENG with optimized structure is implanted into shoe soles portably. It can convert body motion mechanical energy into electric energy and the electrical signal can be used not only as a sensing signal, but also for power to charge micro electronic equipment. Therefore, it can be applied to human body gait balance monitoring, motion frequency monitoring in sport, and so on (as shown in Figure 1a). Figure 1b shows the optical image of TENG with optimized structure. The feature, volume, and structure of TENG with optimized structure can be adjusted by 3D printing technology according to practical needs. The TENG with optimized structure is implanted into sport shoe soles to collect human body mechanical energy data and monitor gait. Figure 1c shows the image of the TENG 3D structure. The key to improving the output performance of TENG is to improve the material and working mode and increase the friction area and friction time. We adopt the same material system; the left side of Figure 1c shows the TENG with regular "sandwich" structure, which is the control object, and the right side of Figure 1c shows the optimized concave-convex structure TENG, which is the experimental object, and the optimized concave-convex structure is fabricated by a 3D printing machine. The TENG with optimized structure can evaluate power generation performance through an increase in friction area and friction time. Figure 1d shows the working mechanism of TENG. No electric charges are generated when the TENG is not driven by mechanical energy (Figure 1d(I)). Then, with the body moving, electric charges occur on the material surface when different two materials make contact (Figure 1d(II)). When the friction layers are separated, the electric potential difference is produced, and the electric charges flow from the bottom layer to the upper layer instantaneously (Figure 1d(III)). When the friction layers depart completely, electric charges are balanced (Figure 1d(IV)). With two friction layers making contact again, the electrostatic induction charge compensates for the electric potential difference through the external load reflux (Figure 1d(V)). The whole portable mobile gait monitor system is shown in Figure 1e. The output electric signals from the triboelectric generator can be collected by oscilloscope, connecting computers to analyse these signals. In addition, irregular AC voltage can be converted to regular DC voltage using a low-frequency stabilized voltage output device. This DC voltage can supply power to devices such as Bluetooth or GPS and the gait can be monitored by these devices. The process of the actual test is shown in Figure S1.

We compare TENG with optimized structure properties with the TENG with regular "sandwich" structure properties (as shown in Figure 2). Figure 2a shows under the force of 11.3 N, the output voltage of two types of TENG at different frequencies. When the frequencies are 0.5 Hz, 1 Hz, and 1.5 Hz, the output voltages of TENG with regular "sandwich" structure are 1.093 V, 0.952 V, and 0.789 V, respectively, whereas the output voltages of TENG with optimized structure are 2.826 V, 2.656 V, and 2.705 V, respectively. It is important to monitor motion frequency for sport sensing monitoring. Body motion frequency and motion complete quality are related to athletic ability. It can be clearly seen from Figure 2a that the voltages of the two TENGs match the tested mechanical frequency, both of which can monitor motion frequency. However, the TENG with optimized structure properties is better than the TENG with regular "sandwich" properties. For proving the TENG with optimized structure properties and showing that it can meet motion mechanical

needs, we test the pressure sensing properties, as shown in Figure 2b. When body motion mechanical energy is collected, the force produced in the human motion is also one of the important links in the transformation of mechanical energy into electric energy. According to Formulations (1) and (2), the landing speed v is calculated (1), then the force in contact with the device is calculated (2) (the default contact time "t" is 0.1 s):

$$\mathrm{mgh} = 1/2 \cdot \mathrm{mv}^2 \quad (1)$$

$$\mathrm{F} = \mathrm{m} \cdot \mathrm{v}/\mathrm{t} \quad (2)$$

Under the frequency of 1 Hz, when the forces are 2.8 N, 11.3 N, and 21.2 N, the output voltages of TENG with regular "sandwich" structure are 0.416 V, 0.732 V, and 1.94 V, respectively whereas the output voltages of TENG with optimized structure are 3.008 V, 4.048 V, and 5 V, respectively. The performance of TENG with optimized structure mechanical energy conversion to electrical energy is obviously better than that of the comparison device. Meanwhile, TENG can sense different motion frequencies and forces. These properties can monitor body gait (frequency) and balance ability (pressure distribution). In order to explore the characteristics of the TENG generator, the energy conversion efficiency of the TENG is investigated. The formulas of energy conversion efficiency are as follows:

$$E_1 = \frac{1}{2}CV^2 \quad (3)$$

$$E_2 = \frac{1}{2}mgh \times n \quad (4)$$

$$\eta = E_1 \div E_2 \times 100\% \quad (5)$$

where E_1 and E_2 represent the electrical energy stored in capacitor and the mechanical energy, respectively. In Formula (3), C and V represent the capacity and charge voltage of capacitor, respectively. m is the mass, g is the gravitational acceleration of the earth's surface, h is the height of the object from the reference plane, and n is the number of workings in Formula (4). In Formula (5), η can be obtained by E_1/E_2, which is the energy conversion efficiency. According to calculation, the energy conversion efficiency of TENG is 0.05%. The capacities of the TENG with and without optimizing in original state are 1.7 nF and 1.5 nF, respectively. The volume of the TENG is ~28 cm^3. The power density is 0.686 mw/m^2, and Table S1 shows the power density compared with other works. Figure 2c shows the testing platform used to test TENGs' properties [48,49]. The stepped motor is used to control motion frequency to imitate human body motion frequency. Through the simple pulley blocks and multiple counterweights, the instant forces exerted on TENGs are calculated. Figure 2d shows the charging of the 4.7 uf capacitor with optimized structure and non-optimized TENG. The working frequency is conducted with 6 Hz for 100 s. When the pressure is 6 N, the optimized TENG is charged to 9.12 V (red line). When the pressure is 3 N, the optimized TENG is charged to 7.52 V (green line). When the pressure is 3 N, the not optimized TENG is charged to 4.24 V (purple line). In Movie S3, the capacitor charges to 16.8 V by TENG at 6 Hz for 100 s (the movie plays at 8× normal speed). Figure 2e shows that TENG drives micro electronic equipment. The capacitor can drive the calculator after being charged by TENG (Figure 2e(i)). Figure 2e(ii) shows a simple demonstration that LEDs are controlled by a Bluetooth module, which is driven by TENG. By tapping TENG, the output voltage drives the Bluetooth transmitter to transmit the information to the receiver. The number and lighting frequency of LEDs on the receiver are directly related to the tapping force and frequency of TENG (Movie S1). This simple wireless information transmission function can provide more potential application scenarios of sport big data.

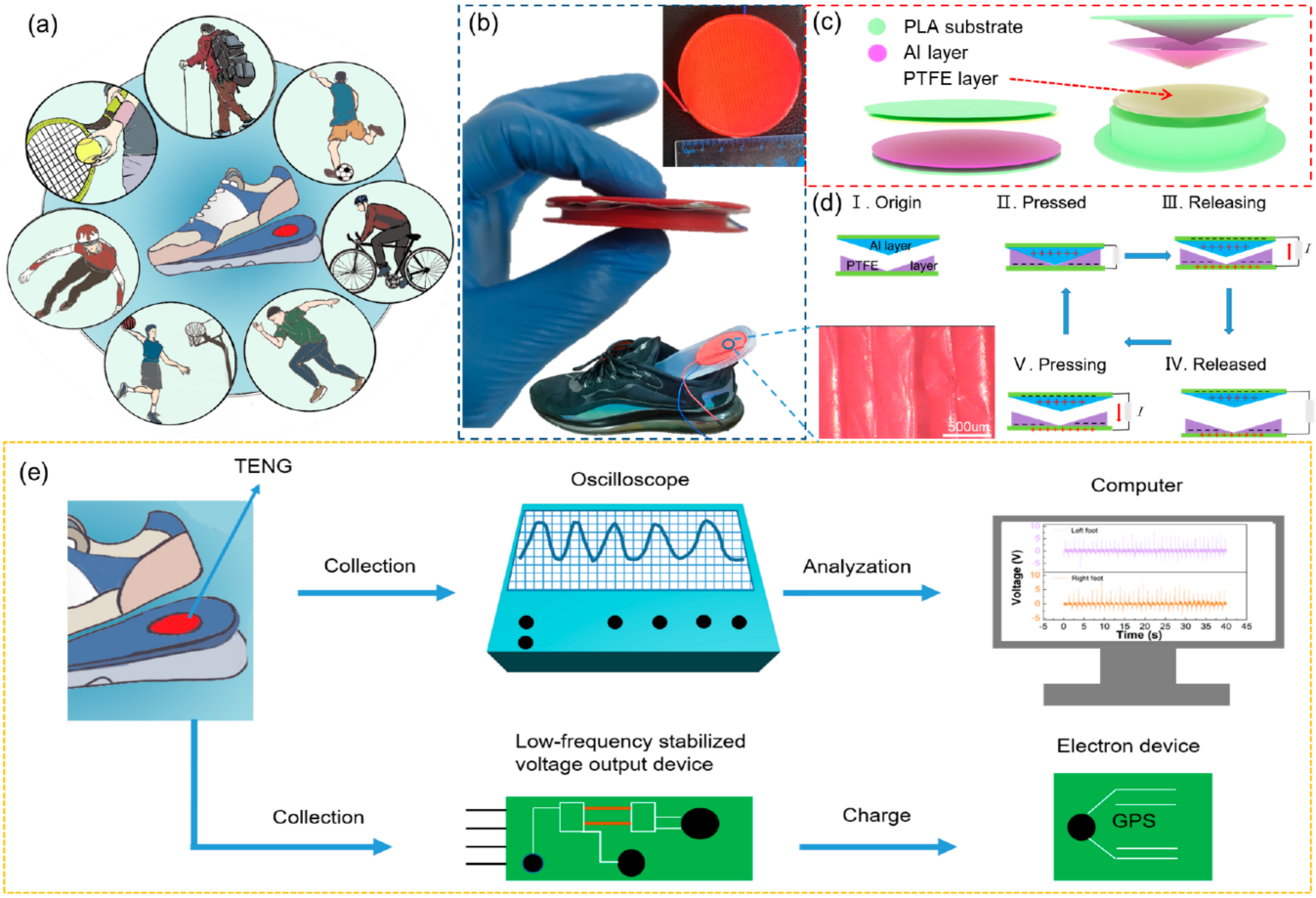

Figure 1. The structure, working mechanism, and application in the sport scene of the portable mobile gait monitor system. (**a**) The practical application of TENG in the sport scene. (**b**) The optical picture and installation position of TENG. (**c**) The structure of TENG. (**d**) The working mechanism of TENG. (**e**) Portable mobile gait monitor system.

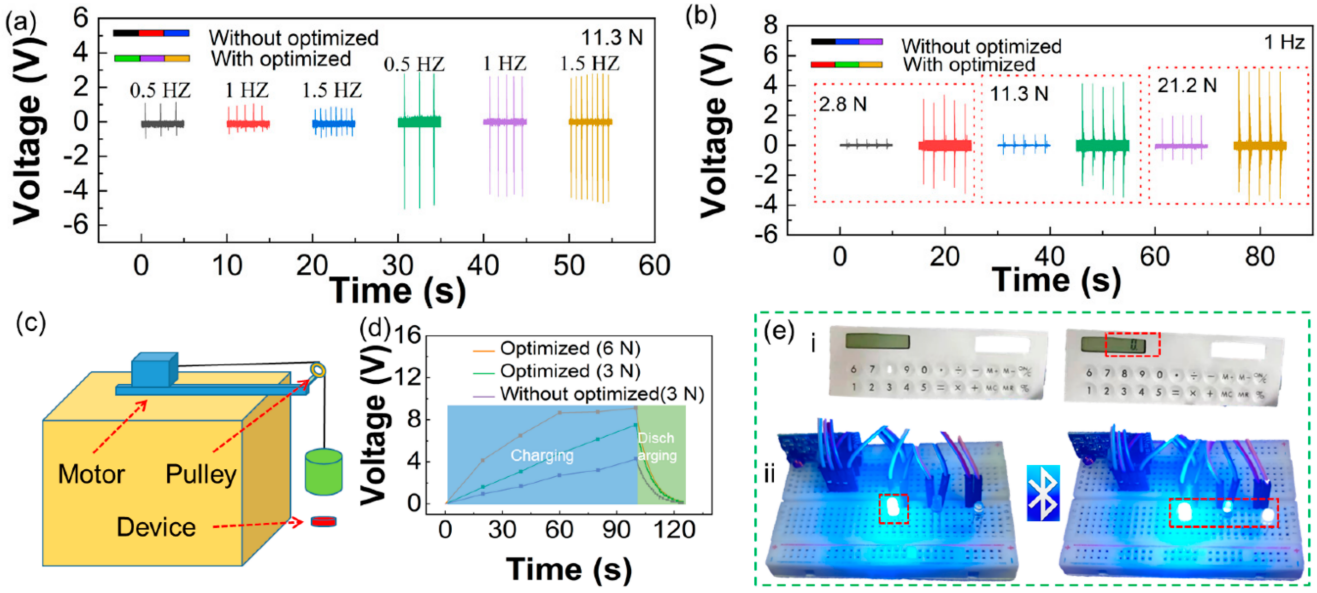

Figure 2. The comparison of properties of TENGs (**a**) The output voltage of TENGs at different frequencies. (**b**) The output voltage of TENGs at different forces. (**c**) The properties' test platform. (**d**) Charging capacitor by TENGs. (**e**) The TENG drives micro electronic equipment.

We find that TENG can collect mechanical energy and convert it into electronic energy to charge the mini capacitor to drive micro electronic equipment in the test process. Moreover, TENG can drive them directly. However, because of irregular voltage output, the high voltage may cause overload damage to micro electronic equipment (such as the GPS module). For improving the application ranges of TENG, we developed a low-frequency voltage stabilizing output device. It supports TENG to drive micro electronic equipment to avoid overloading (as shown in Figure 3). Figure 3a shows the circuit diagram of the low-frequency voltage stabilizing output device. The low frequency voltage stabilizing system consists of six parts: input, rectifier, switch, manostat IC, filter capacitor, and output. The electrical energy is stored in the capacitor through the rectifier bridge. After the capacitor voltage reaches a certain value, the input terminal and the output terminal of DC/DC are connected to make DC/DC work. The output voltage of DC/DC is divided by R1R2, then the DC/DC outputs stable voltage. When the capacitor voltage cannot reach the DC/DC working voltage requirement, DC/DC cuts out with the capacitor and stops outputting, and then the capacitor is charged by the portable mobile gait monitor system again. The TENG internal resistance is 20 MΩ, as shown in Figure S2. Figure S3 shows the one-time test process of AC/DC conversion efficiency. Input voltage and current of AC are 4.5 V and 1.201 A, respectively. The DC output voltage is fixed at 2.87 V and the current is 0.791 A. After five tests, the average of AC input voltage and current are 4.56 V and 1.022 A, respectively. The average output current of DC is 0.784 A, according to the following formula:

$$\eta_{\frac{AC}{DC}} = \frac{P_{input}}{P_{output}} \tag{6}$$

The *AC/DC* conversion efficiency is 48%. Figure 3b shows the low-frequency voltage stabilizing output device working modules. Body motion drives TENG and then TENG collects mechanical energy, outputs triboelectric signals, releases them to DC/DC converter through rectifier bridge and capacitor, and finally achieves the effect of pulse regulated output. Figure 3c shows the output voltage of TENG. Because of irregular mechanical motion, the output voltage ranges from 2 V to 25 V. According to these electrical signals, the gait can be capture and recognized. However, the electrical energy from TENG cannot directly power the electronics, which may cause micro electronic equipment overload and damage due to the overly high and irregular voltage [50–52]. In the future, the portable mobile gait monitor system will be integrated with more functions using a dedicated self-powered ASIC. Through the low-frequency voltage stabilizing output device, the unstable output signal is modulated into a stable output signal. Some microelectronics, such as Bluetooth and GPS mode, can be driven by the portable mobile gait monitor system (as shown in Figure 3d). The voltage switch is controlled by hand operation. When the switch is turned off, the electrical energy output by the triboelectric generator can be stored. When the switch is turned on, a stable DC voltage will be output to supply power for some intelligent monitoring equipment. Figure 3e shows the enlarged view of Figure 3d. In our next work, we will improve the function of the equipment. We want to make it not only stabilize the output, but also meet more motion monitoring possibilities from the judgment and frequency of the electrical signal after the regulated output.

The physiological structure of the human body determines the working mode of the upper and lower limbs. Combined with torso coordination and cooperation, various forms of human movement are formed. With the body movement forms changing, many movements are formed such as push, pull, whip, stretch, swing, and twist, among others. Further, every motion can produce mechanical energy and the mechanical energy is collected by TENG. Figure 4a shows the output voltage of walking collected by the "sandwich" structure TENG, and the average voltage is 0.265 V in 60 s. Figure 4b shows the output voltage of walking collected by TENG with optimized structure, and the average voltage is 5.45 V in 60 s. This shows that both TENGs can collect motion energy and monitor the walking movement. However, the output voltage of TENG with an optimized structure is higher than the "sandwich" structure TENG, which shows that the TENG with

the optimized structure property is better than the "sandwich" structure TENG in body motion energy collection; this result is in line with the testing part. In order to expand more applications in human motion mechanical energy collection and monitoring, the in situ movement and marching movement are tested, which are regular exercises of human body. Figure 4c shows the output voltages of various in situ movements tested by TENG with the optimized structure. When the tester does tiptoe, mark time, and high leg run movements, the output voltages are 2.08 V, 4.16 V, and 29.14 V, respectively. This is because the center of gravity of tiptoe and mark time movements is at the forefoot; however, the TENG is implanted in the heel, which causes the TENG to produce lower voltage. When the tester does high leg run movement, the tester foot makes contact with the ground entirely, so the output voltage is higher than that of the first two motions. The above motion forms are several common forms in in situ movements. We also monitor a variety of sport forms during the march, as shown in Figure 4d. According to the in situ movements' monitoring conclusion, we conclude that the center of gravity shifts and movement ranges determine the output voltage magnitude. Therefore, in the march test, we test from in situ movement to forms of movement in which the center of gravity gradually moves and becomes larger. When the tester does mark time, trot, run, and jump movements, the average output voltages are 4.2 V, 9.78 V, 20.8 V, and 33.14 V, respectively. The above data show that the output voltage of TENG is related to motion forms. The greater the range of human motion forms and the greater the shift of the center of gravity, the more mechanical energy produced and the higher the voltage output.

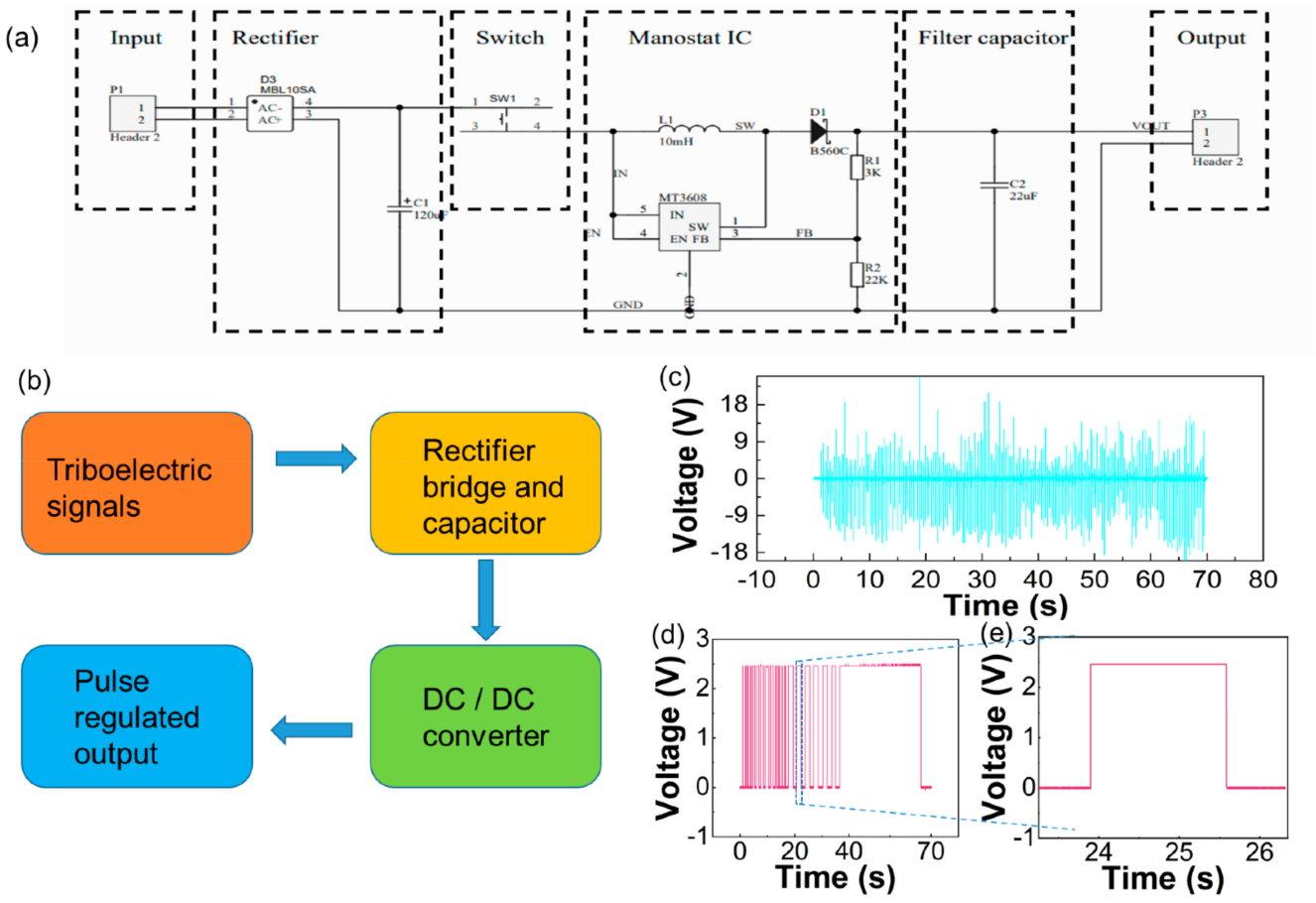

Figure 3. The low-frequency voltage stabilizing output device. (**a**) The circuit diagram of the device. (**b**) The low-frequency voltage stabilizing output device working modules. (**c**) The untreated friction voltage. (**d**) The output voltage of low-frequency voltage stabilizing output device. (**e**) Output details.

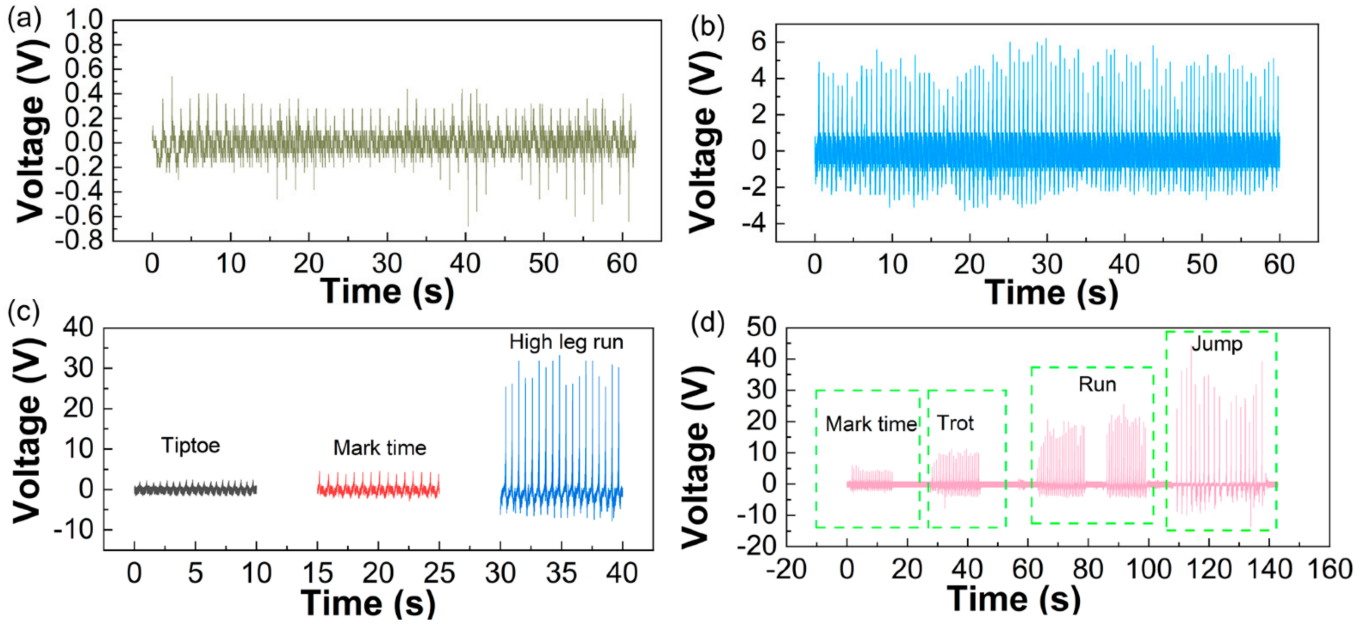

Figure 4. The TENG monitor body motion. (**a**) The output voltage of the TENG with "sandwich" structure. (**b**) The output voltage of TENG with optimized structure. (**c**) The output voltage of the move in situ of TENG. (**d**) The output voltage of the march.

The conclusion of the output voltage of TENG with human body motion forms is drawn in the previous tests. The TENG is used to collect human body motion mechanical energy to drive micro electronic equipment and analyze gait (as shown in Figure 5). Figure 5a shows the output voltage of portable mobile gait monitor system when the tester walks. The average voltages of the first, the second, and the third parts of the left and right feet are 4.5 V, 5.43 V, 5.6 V, 4.91 V, 5.62 V, and 3.47 V, respectively. Through the data and image, we can judge that the left foot is the inertial support leg of the tester. For example, in the start race of 100 m, triple jump, and skiing motions, the tester prefers to use the left leg as an inertial leg with which to move. Figure 5b shows the response of voltages of the first, the second, and the third parts of the left and right feet. The response of the device can be calculated from the following equation:

$$R\% = \left| \frac{V_0 - V_i}{V_i} \right| \times 100\% \quad (7)$$

where the V_0 and V_i respect the output triboelectric voltage at 4.5 V and average voltage of every section. The responses of voltages of the first, the second, and the third parts of the left and right feet are 0%, 19.6%, 19.9%, 17.2%, 8.4%, and 29.8%, respectively. According to the responses of voltage, we can conclude that the gait of the tester is rhythmic. The above data show that the tester's gait cycle is a regular gait with stability, periodicity, and rhythm, and the left leg is the dominant leg. Figure 5c shows the installation position of the portable mobile gait monitor system and the image of portable mobile gait monitor system driving micro electronic equipment. With the human body mechanical energy collection and electronic energy conversion, the portable mobile gait monitor system can drive micro GPS equipment intermittently (as shown in Figure 5d). Move S2 shows the entire testing process. When the tester is running, the portable mobile gait monitor system can collect mechanical energy and convert it into electronic energy to drive micro GPS equipment to launch signal. The signal receiving end can receive the signal and monitor the tester's position in real-time. This kind of application provides a potential application scene for solving the self-demand of electronic equipment in urgent need of power supply or remote areas with weak mobile network signals.

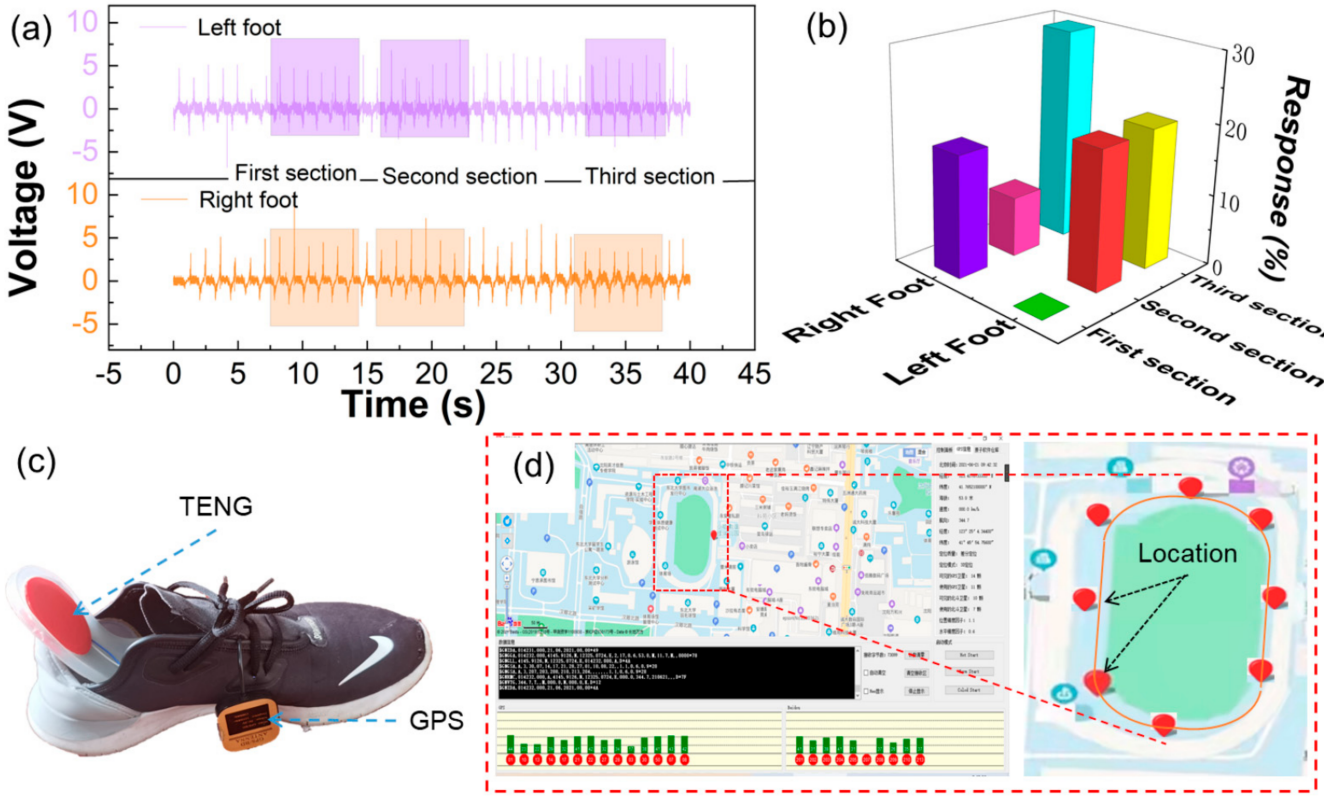

Figure 5. The application of the portable mobile gait monitor system monitor gait balance and driving micro electronic equipment. (**a**) The output voltage of the portable mobile gait monitor system. (**b**) The response of output voltage. (**c**) The portable mobile gait monitor system and micro electronic equipment installation position. (**d**) The e-map of the walking process.

4. Conclusions

In summary, we manufactured a self-powered and portable mobile gait monitor system, which is used to collect body exercise energy and monitor exercise gait and balance ability. The TENG with optimized structure power generation performance was significantly improved by 3D printing technology. TENG is flexibly implanted into a sport shoe to monitor gait and balance in various exercise processes during in situ movement and march movement. The low-frequency voltage stabilizing system can protect micro electronic equipment from overload damage, which is caused by transient high TENG voltage output due to irregular mechanical energy. This interdisciplinary research provides more possibilities for the integrated application of self-powered modular equipment.

Supplementary Materials: The following are available online at https://www.mdpi.com/article/10.3390/en14164996/s1, Movie S1: The self-powered piezoelectric sensor can transmit wireless signal to control the LED, Movie S2: TENG can collect mechanical energy to drive micro GPS equipment to launch signal, Movie S3: TENG charge capacitor, Figure S1: The actual test scenario, Figure S2: The output voltage and power of TENG against different resistance, Figure S3: Single test process of AC/DC conversion efficiency, Table S1: Power density comparison. Table S1: Power density comparison.

Author Contributions: Y.M. and Q.W. put forward the concept of the study. The data were collected, sorted out, and analyzed by T.Z. and Y.Z. T.Z. and C.J. were the supervisors. Y.Z., C.J., X.W. and Y.M. made the verification. X.W., C.J. and Y.Z. made the visualization. Y.M., Q.W. and T.Z. wrote the manuscript. Y.M. and Q.W. finished the writing—comments and editors. All authors have read and agreed to the published version of the manuscript.

Funding: Winter Sports Training monitoring technical services. 2020021300002.

Institutional Review Board Statement: Not applicable.

Informed Consent Statement: Informed consent was obtained from all subjects involved in the study.

Data Availability Statement: The data presented in this study are available on request from the corresponding author.

Conflicts of Interest: The authors declare no conflict of interest. The funders had no role in the design of the study; in the collection, analyses, or interpretation of data; in the writing of the manuscript; or in the decision to publish the results.

References

1. Steven, C.; Arun, M. Opportunities and challenges for a sustainable energy future. *Nature* **2012**, *7411*, 294–303.
2. Maeng, J.; Park, I.; Shim, M.; Jeong, J.; Kim, C. A High-Voltage Dual-Input Buck Converter with Bidirectional Inductor Current for Triboelectric Energy-Harvesting Applications. *IEEE J. Solid-State Circ.* **2021**, *56*, 541–553. [CrossRef]
3. Quelen, A.; Morel, A.; Gasnier, P.; Grezaud, R.; Monfray, S.; Pillonnet, G. A 30 nA Quiescent 80 nW-to-14 mW Power-Range Shock-Optimized SECE-Based Piezoelectric Harvesting Interface with 420% Harvested-Energy Improvement. *ISSCC* **2018**, *2018*, 150–152.
4. Morel, A.; Quelen, A.; Berlitz, C.A.; Gibus, D.; Pillonnet, G. 32.2 Self-Tunable Phase-Shifted SECE Piezoelectric Energy-Harvesting IC with a 30nW MPPT Achieving 446% Energy-Bandwidth Improvement and 94% Efficiency. In Proceedings of the 2020 IEEE International Solid-State Circuits Conference—(ISSCC), San Francisco, CA, USA, 16–20 February 2020.
5. Lee, R. The Outlook for Population Growth. *Science* **2011**, *333*, 569–573. [CrossRef] [PubMed]
6. Zhu, G.; Peng, B.; Chen, J.; Jing, Q.; Wang, Z.L. Triboelectric nanogenerators as a new energy technique: From fundamentals, devices, to applications. *Nano Energy* **2015**, *14*, 126–138. [CrossRef]
7. Chen, J.; Huang, Y.; Zhang, N.; Zou, H.; Liu, R.; Tao, C.; Fan, X.; Wang, Z.L. Micro-cable structured textile for simultaneously harvesting solar and mechanical energy. *Nat. Energy* **2016**, *1*, 16138. [CrossRef]
8. Wang, J.; Li, X.; Zi, Y.; Wang, S.; Li, Z.; Zheng, L.; Yi, F.; Li, S.; Wang, Z.L. A Flexible Fiber-Based Supercapacitor–Triboelectric-Nanogenerator Power System for Wearable Electronics. *Adv. Mater.* **2015**, *27*, 4830–4836. [CrossRef]
9. Chandrasekhar, A.; Alluri, N.R.; Vivekananthan, V.; Purusothaman, Y.; Kim, S.J. A sustainable freestanding biomechanical energy harvesting smart backpack as a portable-wearable power source. *J. Mater. Chem. C* **2017**, *5*, 1488–1493. [CrossRef]
10. Zhu, M.; Huang, Y.; Ng, W.S.; Liu, J.; Wang, Z.; Wang, Z.; Hu, H.; Zhi, C. 3D spacer fabric based multifunctional triboelectric nanogenerator with great feasibility for mechanized large-scale production. *Nano Energy* **2016**, *27*, 439–446. [CrossRef]
11. Ji, S.H.; Cho, Y.S.; Yun, J.S. Wearable Core-Shell Piezoelectric Nanofiber Yarns for Body Movement Energy Harvesting. *Nanomaterials* **2019**, *9*, 555. [CrossRef]
12. Zhu, J.; Wang, X.; Xing, Y.; Li, J. Highly Stretchable All-Rubber-Based Thread-Shaped Wearable Electronics for Human Motion Energy-Harvesting and Self-Powered Biomechanical Tracking. *Nanoscale Res. Lett.* **2019**, *14*, 247. [CrossRef] [PubMed]
13. Mao, Y.; Zhang, W.; Wang, Y.; Guan, R.; Liu, B.; Wang, X.; Sun, Z.; Xing, L.; Chen, S.; Xue, X. Self-Powered Wearable Athletics Monitoring Nanodevice Based on ZnO Nanowire Piezoelectric-Biosensing Unit Arrays. *Sci. Adv. Mater.* **2019**, *11*, 351–359. [CrossRef]
14. Mao, Y.; Shen, M.; Liu, B.; Xing, L.; Chen, S.; Xue, X. Self-Powered Piezoelectric-Biosensing Textiles for the Physiological Monitoring and Time-Motion Analysis of Individual Sport. *Sensors* **2019**, *19*, 3310. [CrossRef]
15. Mao, Y.; Ba, N.; Gao, X.; Wang, Z.; Shen, M.; Liu, B.; Li, B.; Ma, X.; Chen, S. Self-Powered Wearable Sweat-Lactate Analyzer for Scheduling Training of Boat Race. *J. Nanoelectron. Optoelectron.* **2020**, *15*, 212–218. [CrossRef]
16. Mao, Y.; Yue, W.; Zhao, T.; Shen, M.; Chen, S. A Self-Powered Biosensor for Monitoring Maximal Lactate Steady State in Sport Training. *Biosensors* **2020**, *10*, 75. [CrossRef]
17. Mao, Y.; Zhu, Y.; Zhao, T.; Jia, C.; Bian, M.; Li, X.; Liu, Y.; Liu, B. A Portable and Flexible Self-Powered Multifunctional Sensor for Real-Time Monitoring in Swimming. *Biosensors* **2021**, *11*, 147. [CrossRef] [PubMed]
18. Liu, W.; Wang, Z.; Wang, G.; Liu, G.; Chen, J.; Pu, X.; Xi, Y.; Wang, X.; Guo, H.; Hu, C. Integrated charge excitation triboelectric nanogenerator. *Nat. Commun.* **2019**, *10*, 1426. [CrossRef]
19. Chen, C.; Zhang, L.; Ding, W.; Chen, L.; Yu, W. Woven Fabric Triboelectric Nanogenerator for Biomotion Energy Harvesting and as Self-Powered Gait-Recognizing Socks. *Energies* **2020**, *13*, 4119. [CrossRef]
20. Shi, H.; Liu, Z.; Mei, X. Overview of Human Walking Induced Energy Harvesting Technologies and Its Possibility for Walking Robotics. *Energies* **2019**, *13*, 86. [CrossRef]
21. Kong, D.S.; Han, J.Y.; Ko, Y.J.; Park, S.H.; Lee, M.; Jung, J.H. A Highly Efficient and Durable Kirigami Triboelectric Nanogenerator for Rotational Energy Harvesting. *Energies* **2021**, *14*, 1120. [CrossRef]
22. Zhou, Y.; Shen, M.; Cui, X.; Shao, Y.; Zhang, Y. Triboelectric Nanogenerator Based Self-powered Sensor for Artificial Intelligence. *Nano Energy* **2021**, *84*, 105887. [CrossRef]
23. Zhang, H.; Zhang, P.; Zhang, W. A high-output performance mortise and tenon structure triboelectric nanogenerator for human motion sensing. *Nano Energy* **2021**, *84*, 105933. [CrossRef]
24. Zhang, J.; Zhang, Y.; Sun, N.; Li, Y.; Du, J.; Zhu, L.P.; Hao, X.H. Enhancing output performance of triboelectric nanogenerator via large polarization difference effect. *Nano Energy* **2021**, *84*, 105892. [CrossRef]

25. Chen, B.; Yang, Y.; Wang, Z.L. Scavenging Wind Energy by Triboelectric Nanogenerators. *Adv. Energy Mater.* **2018**, *8*, 1702649. [CrossRef]
26. Cho, S.; Hanif, Z.; Yun, Y.; Khan, Z.A.; Choi, D. Triboelectrification-driven Microbial Inactivation in a Conductive Cellulose Filter for Affordable, Portable, and Efficient Water Sterilization. *Nano Energy* **2021**, *88*, 106228. [CrossRef]
27. Yun, Y.; Jang, S.; Cho, S.; Lee, S.H.; Hwang, H.J.; Choi, D. Exo-shoe triboelectric nanogenerator: Toward high-performance wearable biomechanical energy harvester. *Nano Energy* **2021**, *80*, 105525. [CrossRef]
28. Ma, L.; Zhou, M.; Wu, R.; Patil, A.; Gong, H.; Zhu, S.; Wang, T.; Zhang, Y.; Shen, S.; Dong, K.; et al. Continuous and Scalable Manufacture of Hybridized Nano-Micro Triboelectric Yarns for Energy Harvesting and Signal Sensing. *ACS Nano* **2020**, *14*, 4716–4726. [CrossRef]
29. Chen, C.; Guo, H.; Chen, L.; Wang, Y.; Pu, X.; Yu, W.; Wang, F.; Du, Z.; Wang, Z.L. Direct Current Fabric Triboelectric Nanogenerator for Biomotion Energy Harvesting. *ACS Nano* **2020**, *14*, 4585–4594. [CrossRef]
30. Fan, F.; Tang, W.; Wang, Z.L. Flexible Nanogenerators for Energy Harvesting and Self-Powered Electronics. *Adv. Mater.* **2016**, *28*, 4283–4305. [CrossRef] [PubMed]
31. He, C.; Zhu, W.; Gu, G.; Jiang, T.; Xu, L.; Chen, B.; Han, C.; Li, D.; Wang, Z. Integrative square-grid triboelectric nanogenerator as a vibrational energy harvester and impulsive force sensor. *Nano Res.* **2018**, *11*, 1157–1164. [CrossRef]
32. Jiang, D.; Ouyang, H.; Shi, B.; Zou, Y.; Tan, P.; Qu, X.; Chao, S.; Xi, Y.; Zhao, C.; Fan, Y.; et al. A wearable noncontact free-rotating hybrid nanogenerator for self-powered electronics. *InfoMat* **2020**, *2*, 1191–1200. [CrossRef]
33. Ni, G.L.; Zhu, X.S.; Mi, H.Y.; Feng, P.Y.; Li, J.; Jing, X.; Dong, B.B.; Liu, C.T.; Shen, C.Y. Skinless Porous Films Generated by Supercritical CO 2 Foaming for High-Performance Complementary Shaped Triboelectric Nanogenerators and Self-Powered Sensors. *Nano Energy* **2021**, *87*, 106148. [CrossRef]
34. Wu, C.; Kim, T.W.; Park, J.H.; An, H.; Shao, J.; Chen, X.; Wang, Z.L. Enhanced Triboelectric Nanogenerators Based on MoS 2 Monolayer Nanocomposites Acting as Electron-Acceptor Layers. *ACS Nano* **2017**, *11*, 8356–8368. [CrossRef] [PubMed]
35. GBD 2017 Causes of Death Collaborators. Global, regional, and national age-sex-specific mortality for 282 causes of death in 195 countries and territories, 1980-2017: A systematic analysis for the Global Burden of Disease Study 2017. *Lancet* **2018**, *392*, 1736–1788. [CrossRef]
36. GBD 2017 DALYs and HALE Collaborators. Global, regional, and national disability-adjusted life-years (DALYs) for 359 diseases and injuries and healthy life expectancy (HALE) for 195 countries and territories, 1990–2017: A systematic analysis for the Global Burden of Disease Study 2017. *Lancet* **2018**, *392*, 1859–1922. [CrossRef]
37. GBD 2017 Mortality Collaborators. Global, regional, and national age-sex-specific mortality and life expectancy, 1950–2017: A systematic analysis for the Global Burden of Disease Study 2017. *Lancet* **2018**, *392*, 1684–1735. [CrossRef]
38. Zhou, M.; Wang, H.; Zhu, J.; Chen, W.; Wang, L.; Liu, S.; Li, Y.; Wang, L.; Liu, Y.; Yin, P.; et al. Cause-specific mortality for 240 causes in China during 1990–2013: A systematic subnational analysis for the Global Burden of Disease Study 2013. *Lancet* **2016**, *387*, 251–272. [CrossRef]
39. Sherrington, C.; Fairhall, N.J.; Wallbank, G.K.; Tiedemann, A.; Michaleff, Z.A.; Howard, K.; Clemson, L.; Hopewell, S.; Lamb, S.E. Exercise for preventing falls in older people living in the community. *Cochrane Db. Syst. Rev.* **2019**, *1*, CD012424. [CrossRef]
40. Gardner, M.M.; Robertson, M.G.; Campbell, A.J. Exercise in preventing falls and fall related injuries in older people: A review of randomised controlled trials. *Br. J. Sport Med.* **2000**, *34*, 7–17. [CrossRef]
41. Rau, C.S.; Lin, T.S.; Wu, S.C.; Yang, J.C.S.; Hsu, S.Y.; Cho, T.Y.; Hsieh, C.H. Geriatric hospitalizations in fall-related injuries. *Scand. J. Trauma Resusc. Emerg. Med.* **2014**, *22*, 63. [CrossRef] [PubMed]
42. Schwendimann, R.; Buhler, H.; Geest, S.D.; Milisen, K. Falls and consequent injuries in hospitalized patients: Effects of an interdisciplinary falls prevention program. *BMC Health Serv. Res.* **2006**, *6*, 69. [CrossRef] [PubMed]
43. Shier, V.; Trieu, E.; Ganz, D.A. Implementing exercise programs to prevent falls: Systematic descriptive review. *Inj. Epidemiol.* **2016**, *3*, 1–18. [CrossRef] [PubMed]
44. Kutcher, J.S.; McCRory, P.; Davis, G.; Ptito, A.; Meeuwisse, W.H.; Broglio, S.P. What evidence exists for new strategies or technologies in the diagnosis of sport concussion and assessment of recovery. *Br. J. Sport Med.* **2013**, *47*, 299–303. [CrossRef]
45. Ahmadi, A.; Mitchell, E.; Richter, C.; Estelle, F.D.; Gowing, M.; O'Connor, N.E.; Moran, K. Toward Automatic Activity Classification and Movement Assessment During a Sport Training Session. *IEEE Internet Things J.* **2017**, *2*, 23–32. [CrossRef]
46. Fan, F.; Lin, L.; Zhu, G.; Wu, W.; Zhang, R.; Wang, Z.L. Transparent Triboelectric Nanogenerators and Self-Powered Pressure Sensors Based on Micropatterned Plastic Films. *Nano Lett.* **2012**, *12*, 3109–3114. [CrossRef] [PubMed]
47. Zeng, H.; He, H.X.; Fu, Y.M.; Zhao, T.M.; Han, W.X.; Xing, L.L.; Zhang, Y.; Zhan, Y.; Xue, X.Y. A self-powered brain-linked biosensing electronic-skin for actively tasting beverage and its potential application in artificial gustation. *Nanoscale* **2018**, *10*, 19987–19994. [CrossRef]
48. Zhao, T.M.; Zheng, C.W.; He, H.X.; Guan, H.Y.; Zhong, T.Y.; Xing, L.L.; Xue, X.Y. A self-powered biosensing electronic-skin for real-time sweat Ca2+ detection and wireless data transmission. *Smart Mater. Struct.* **2019**, *28*, 085015. [CrossRef]
49. Zhao, T.M.; Li, J.L.; Zeng, H.; Fu, Y.M.; He, H.X.; Xing, L.L.; Zhang, Y.; Xue, X.Y. Self-powered wearable sensing-textiles for real-time detecting environmental atmosphere and body motion based on surface-triboelectric coupling effect. *Nanotechnology* **2018**, *29*, 405504. [CrossRef]

50. Li, Y.J.; Morel, A.; Gallant, D.; Mauzeroll, J. Ag+ Interference from Ag/AgCl Wire Quasi-Reference Counter Electrode Inducing Corrosion Potential Shift in an Oil-Immersed Scanning Micropipette Contact Method Measurement. *Anal. Chem.* **2021**, *93*, 9657–9662. [CrossRef]
51. Morel, A.; Quelen, A.; Gasnier, P.; Grezaud, R.; Monfray, S.; Badel, A.; Pillonnet, G. A Shock-Optimized SECE Integrated Circuit. *IEEE J. Solid-State Circ.* **2018**, *53*, 3420–3433. [CrossRef]
52. Roussel, C.; Morel, A.; Dussiott, M.; Marin, M.; Colard, M.; Fricot-Monsinjon, A.; Martinez, A.; Chambrion, C.; Henry, B.; Casimir, M.; et al. Rapid clearance of storage-induced microerythrocytes alters transfusion recovery. *Blood* **2021**, *137*, 2285–2298. [CrossRef] [PubMed]